Scanning tunneling microscopy investigations of the surface structure and electronic properties of ternary graphite intercalation compounds

Stephen P. Kelty and Charles M. Lieber
Department of Chemistry, Columbia University, New York, New York 10027

(Received 24 July 1990; accepted 31 August 1990)

Scanning tunneling microscopy has been used to characterize the surface structure of the $KHgC_4$ (stage 1) and $KHgC_8$ (stage 2) graphite intercalation compounds. Images of the stage 1 and stage 2 materials exhibit a new commensurate 2×2 superlattice in addition to the centered hexagonal lattice observed in images of pristine graphite. Consideration of the intercalant layer structure and previous studies of stage 1 (MC_8) and stage 2 (MC_{24}) alkali metal graphite intercalation compounds (GICs) indicate that the 2×2 superlattice is due to a modulation of the surface carbon layer density of states by the periodic (2×2) potential of the potassium ions. In addition, a new orthorhombic superlattice, $\mathbf{a} = \mathbf{b} = 0.89$ nm and $< \mathbf{a} - \mathbf{b} = 89°$, has been observed in images of the stage 1 $KHgC_4$ material. Possible origins of this novel superstructure are discussed.

I. INTRODUCTION

Scanning tunneling microscopy (STM) images of the surface of graphite often exhibit anomalous features such as a large asymmetry between adjacent surface carbon atom sites, and a large vertical corrugation between the atomic positions and the centers of the carbon rings.[1-8] Theoretical studies have suggested that the observed asymmetry between adjacent carbon atoms is due to the intrinsic differences in the electronic states of these two sites.[6-8] These differences arise from the *AB* stacking sequence of hexagonal graphite. The large[9] corrugation amplitude observed in images has also been attributed to the electronic properties of graphite.[2] Specifically, nodes in the surface wave function arising from the small size and hexagonal symmetry of the Fermi surface could yield anomalously high corrugations. STM studies of graphite intercalation compounds (GICs) should provide an ideal experimental test for these theoretical explanations of the anomalous features in images of graphite since the carbon layer stacking sequence and the size of the Fermi surface can be varied through intercalation of different electron donor and acceptor species.[10,11]

Indeed, there have recently been several high-resolution STM studies of stage 1 (MC_8)[12-14] and stage-2 (MC_{24})[13] alkali metal GICs. The carbon layer stacking sequence is *AA* in the stage 1 materials and *AABBCCA*$\cdots$ in the stage 2 compounds. In addition, charge-transfer from the alkali metal layers to the carbon layers in both materials significantly expands the Fermi surface relative to graphite.[10] The STM images of the MC_8 GICs show a new $2\mathbf{a}\times2\mathbf{a}$ ($\mathbf{a} = 0.246$ nm) superlattice and the images of the MC_{24} materials exhibit the centered hexagonal structure ($\mathbf{a} = 0.246$ nm) observed for pristine graphite in contrast to theoretical predictions.[6-8,15] To probe further the origin of these fascinating results and to understand better the surface properties of GICs in general we have extended our investigation to include the ternary GICs, $M_xM'_yC_n$, and herein we report the first atomic resolution STM images of stage 1 $KHgC_4$ and stage 2 $KHgC_8$.

II. EXPERIMENT

The stage 1 and stage 2 $KHgC_n$ GICs were prepared by heating KHg and thin highly oriented pyrolytic graphite crystals (A. W. Moore, Union Carbide, Inc.) in sealed Pyrex tubes at 200 and 300 °C, respectively. The phase purity of the GICs was determined by analysis of 001 diffraction lines. The pink stage 1 compound had a *c*-axis repeat (I_c) of 1.021 nm while I_c for the blue stage 2 material was 1.355 nm; these data are consistent with previous studies of pure stage 1 α-phase and ordered stage 2 materials.[11,16,17]

The STM measurements were made in an inert atmosphere glove box using a commercial instrument (Nanoscope, Digital Instruments, Santa Barbara, CA). The images were recorded using Pt–Ir alloy (80%–20%) tips on freshly cleaved sample surfaces; these surfaces were stable for at least 12 hours in the glove-box. Numerous STM tips and $KHgC_4$ and $KHgC_8$ crystals were investigated in these studies, and the images reported below are typical of several hundred obtained on these materials. Furthermore, these images were recorded on areas that did not exhibit surface steps or grain boundaries, and hence we believe that these images are characteristic of the intrinsic properties of the crystal surface and are not due to anomalies associated with crystal defects.[18,19]

III. RESULTS AND DISCUSSION

Diffraction studies of the stage 1 $KHgC_4$ material have shown that the intercalant layer can adopt two distinct orientations in the crystal; these are termed the α and β phases.[16,17] In the present investigation we focus only on pure stage 1 α-phase and stage 2 crystals. The structure of the carbon and intercalant layers of these materials is shown schematically in Fig. 1. A key point to recognize in this figure is that the potassium layer, which lies directly beneath the carbon layer, forms an ordered 2×2 superlattice in both the stage 1 α-phase and stage 2 crystals. Notably, this 2×2

 0734-211X/91/021068-04$01.00

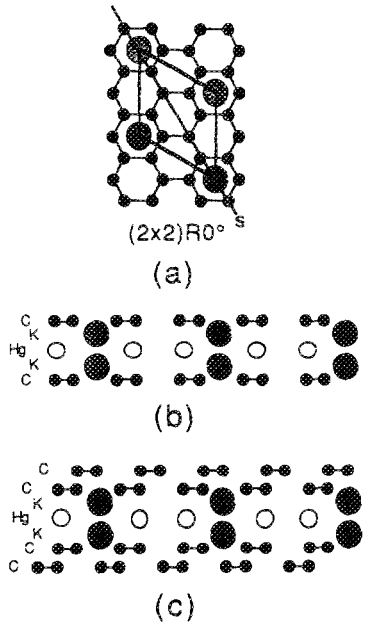

FIG. 1. Schematic views of the structures of the $KHgC_4$ and $KHgC_8$ GICs. (a) Top-view showing a projection of a carbon layer and the commensurate 2×2 potassium layer. The 2×2 structure is adopted by the potassium layer in both $KHgC_4$ and $KHgC_8$. (b) Side-view of $KHgC_4$ indicating the stacking sequence of the carbon, potassium, and mercury layers. (c) Side-view of $KHgC_8$ showing the stacking sequence of the carbon, potassium, and mercury layers. The cross section views in (b) and (c) were taken along the line (a) marked "*s*".

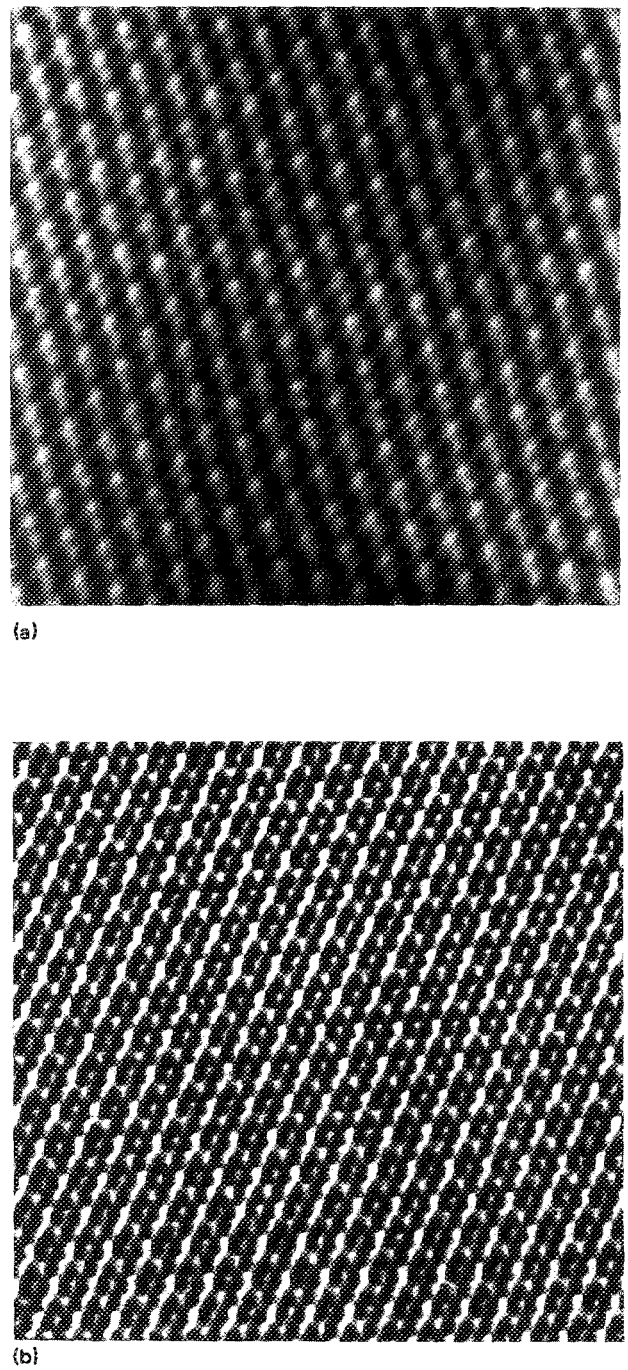

FIG. 2. (a) 8.0×8.0-nm^2 image of $KHgC_4$ recorded with a bias voltage of -15 mV and a tunneling current of 6 nA. (b) 8.0×8.0-nm^2 image of $KHgC_8$ recorded with a bias voltage of 25 mV and a tunneling current of 4 nA. Both images exhibit a 2×2 modulation of the hexagonal structure observed in images of graphite.

superlattice is the same as that found in the stage 1 MC_8 GICs.

Gray-scale STM images of the stage 1 and stage 2 materials are shown in Fig. 2. The image of $KHgC_4$ is typical of that observed over 90%–95% of the surface while the image of $KHgC_8$ is representative of all of the data obtained to date on the stage 2 materials. Images of both the stage 1 and stage 2 materials exhibit a $2a\times2a$ superlattice and the centered hexagonal structure typical of pristine graphite; the 2×2 superlattice is commensurate with the hexagonal graphite lattice. Similar features were observed in images recorded with bias-voltages from -750 to $+750$ mV and with tunneling currents from 0.5 to 6 nA. Furthermore, images recorded in the constant height mode, where the force between the tip and sample are nearly constant, are essentially the same as the constant current topographs. In addition, we note that the 2×2 superlattice and hexagonal graphite lattice observed in images of $KHgC_4$ and $KHgC_8$ have the same features observed previously in images of the stage 1 MC_8 (M = K, Rb, Cs) GICs.[12,13]

Several explanations could account for the 2×2 structure observed in our images of $KHgC_n$ GICs. First, as suggested for the stage 1 alkali metal materials[14] it is possible that the 2×2 structure corresponds to a direct image of the K atoms on the surface. The absence of lattice defects (e.g., missing K atoms) and the high stability of this structure (>12 h in the glove box) argue against the presence of a reactive K layer on top of the surface. Second, it is possible that changes in the Fermi level, which are due to charge transfer from potassium to the carbon layers, could lead to the formation of a 2a charge density wave.[13] This explanation is also unlikely since the same 2×2 superlattice is observed in images of $KHgC_4$ and $KHgC_8$ even though the degree of charge transfer to the carbon layers differs significantly in these two GICs. We believe that the most reasonable explanation for the 2×2 superlattice is that it is due to an electronic effect of the ordered potassium ions directly beneath the surface carbon layer. Specifically, the periodic (2×2) potential of the

potassium ions modulates the density of states of the surface carbon layer to produce the observed 2×2 superlattice. A 2×2 ordered array of alkali metal ions is known to exist in $KHgC_4$, $KHgC_8$, and the MC_8 GICs. Additionally, the absence of a 2×2 superstructure in images of the stage 2 MC_{24} materials is consistent with these results since the alkali metal layers are disordered at room temperature in these GICs.

We have also characterized a new orthorhombic superlattice ($\mathbf{a} = \mathbf{b} = 0.89$ nm, $<\mathbf{a} - \mathbf{b} = 89° \pm 2°$) in images of the stage 1 $KHgC_4$ GIC (Fig. 3). We believe that the orthorhombic symmetry of this superstructure is intrinsic and not due to an asymmetric tip or piezo nonlinearities since the underlying graphite lattice is hexagonal. The superlattice is observed in two distinct orientations ($5° \pm 2°$ and $13° \pm 1°$) relative to the underlying graphite lattice. These orientations are highlighted by lines in Fig. 3. The 0.89-nm period superstructure is found over 5%–10% of the surface, and has never been observed simultaneously with the 2×2 superlattice discussed above. This superlattice is, however, observed immediately after $KHgC_4$ crystals are cleaved and is stable for at least 12 hours; hence, it is unlikely that 0.89-nm period superstructure evolves in time from the 2×2 superlattice.

The origin of this new orthorhombic superlattice in $KHgC_4$ is not well-understood at present. Modulation of the carbon layer density of states by a dilute potassium layer (in analogy to the 2×2 superlattice) is unlikely since previous surface analytical studies have shown that the surface donor intercalant concentrations are either the same or higher than in the bulk.[20] The possibility that this 0.89-nm superstructure is due to a rotational moire pattern[19] is also unlikely since this pattern should have hexagonal symmetry in contrast to the observed orthorhombic structure. One other possible explanation for this new superlattice is that it is due to the charge density wave that has been postulated for the β-phase of $KHgC_4$.[16] Additional studies are now in progress to test this interesting suggestion.

Last, it is important to note that in addition to the new superlattices only alternate surface carbon atom sites are observed in our images of $KHgC_4$ and $KHgC_8$. Since the stacking sequence and Fermi surface size change significantly in these materials our data contrast the results expected based on theoretical models proposed to explain the carbon site asymmetry and vertical corrugations in graphite. Hence, additional theoretical and experimental studies are certainly warranted so that a better understanding of the factors that determine observed images in these layered materials can be developed.

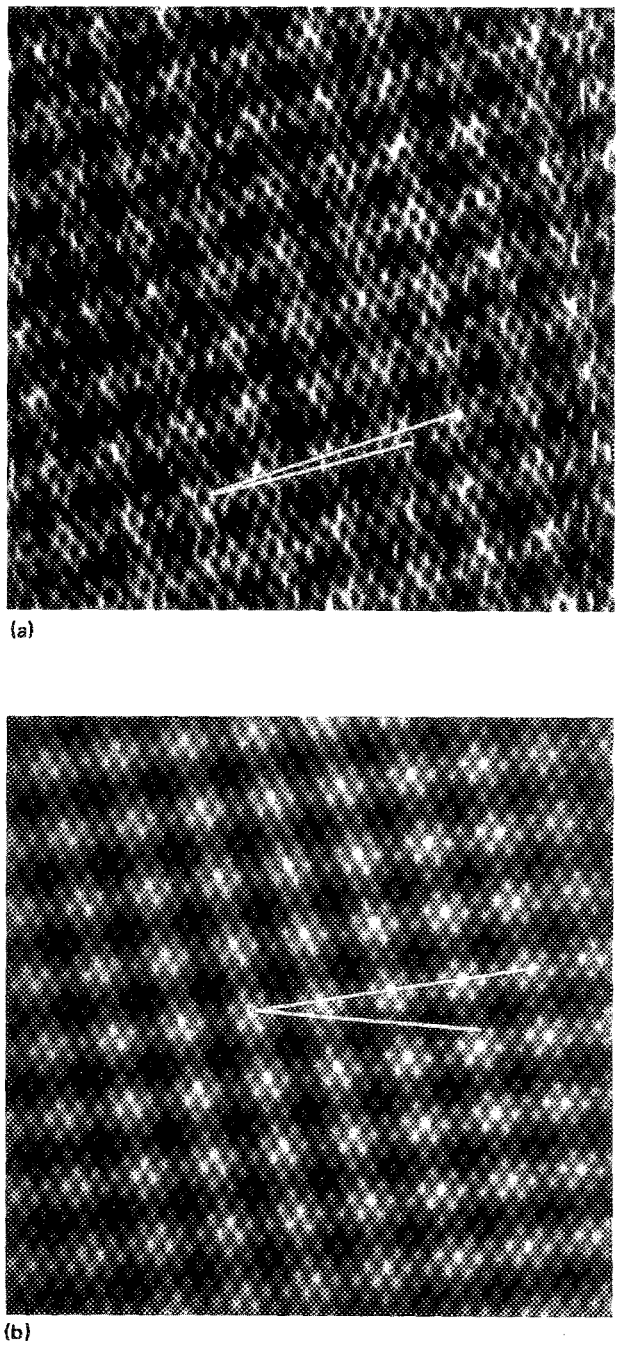

FIG. 3. (a) 8.0×8.0-nm^2 image of $KHgC_4$ recorded with a bias voltage of 15 mV and a tunneling current of 4 nA that shows the 0.89-nm period orthorhombic superlattice. The superlattice is oriented at an angle of $5° \pm 1°$ relative to the hexagonal graphite structure. (b) 8.0×8.0-nm^2 image of the 0.89-nm period superlattice which is oriented at an angle of $13° \pm 1°$ relative to the hexagonal graphite structure. The orientation of the orthorhombic superlattice is highlighted by lines in (a) and (b).

IV. CONCLUSIONS

In summary, we have used STM to characterize the surface structure of stage 1 $KHgC_4$ and stage 2 $KHgC_8$. Images of the stage 1 and stage 2 materials exhibit a commensurate 2×2 superlattice in addition to the centered hexagonal lattice observed in images of pristine graphite. Consideration of the intercalant layer structure and previous studies of stage 1 MC_8 and stage 2 MC_{24} alkali metal GICs indicates that the 2×2 superlattice is due to a modulation of the surface carbon layer density of states by the periodic (2×2) potential of the potassium ions. In addition, a new orthorhombic superlattice, $\mathbf{a} = \mathbf{b} = 0.89$ nm and $<\mathbf{a} - \mathbf{b} = 89°$, has been observed in images of the stage 1 $KHgC_4$ material. At present the most likely explanation of this 0.89 nm period superlattice is that it is due to an incommensurate charge density wave, although additional studies are clearly needed to prove this proposal.

ACKNOWLEDGMENTS

The authors thank A. W. Moore (Union Carbide) for generously providing HOPG samples. S.P.K was supported by a NIH-NRSA graduate fellowship. C.M.L acknowledges support of this work by the National Science and David and Lucile Packard Foundations

[1] G. Binnig, H. Fuchs, Ch. Gerber, H. Rohrer, E. Stoll, and E. Tosatti, Europhys. Lett **1**, 31 (1986).
[2] J. Tersoff, Phys. Rev. Lett. **57**, 440 (1986).
[3] J. M. Soler, A. M. Baro, N. Garcia, and H. Rohrer, Phys. Rev. Lett. **57**, 444 (1986).
[4] H. J. Mamin, E. Ganz, D. W. Abraham, R. E. Thomson, and J. Clarke, Phys. Rev. B **34**, 9015 (1986).
[5] J. B. Pethica, Phys. Rev. Lett. **57**, 3235 (1986).
[6] I. P. Batra, N. Garcia, H. Rohrer, H. Salemink, E. Stoll, and S. Ciraci, Surf. Sci. **181**, 126 (1987).
[7] D. Tomanek, S. G. Louie, H. J. Mamin, D. W. Abraham, R. E. Thomson, E. Ganz, and J. Clarke, Phys. Rev. B **35**, 7790 (1987).
[8] D. Tomanek and S. G. Louie, Phys. Rev. B **37**, 8327 (1988).
[9] The "large" corrugation amplitudes (≈ 1 Å) are to be distinguished from "giant" corrugations[4] that are probably caused by elastic interactions between the tip and surface.
[10] M. S. Dresselhaus and G. Dresselhaus, Adv. Phys. **30**, 139 (1981).
[11] S. A. Solin and H. Zabel, Adv. Phys. **37**, 87 (1988).
[12] S. P. Kelty and C. M. Lieber, J. Phys. Chem. **93**, 5983 (1989).
[13] S. P. Kelty and C. M. Lieber, Phys. Rev. B **40**, 5856 (1989).
[14] D. Anselmetti, R. Wiesendanger, and H. J. Guntherodt, Phys. Rev. B **39**, 11135 (1989).
[15] X. Qin and G. Kirczenow, Phys. Rev. B **41**, 4976 (1990).
[16] A. Chaiken, M. S. Dresselhaus, T. P. Orlando, G. Dresselhaus, P. M. Tedrow, D. A. Neumann and W. A. Kamitahara, Phys. Rev. B **41**, 71 (1990).
[17] L. E. DeLong and P. C. Eklund, Synth. Met. **5**, 291 (1983).
[18] H. A. Mizes and J. S. Foster, Science **244**, 559 (1989).
[19] M. Kuwabara, D. R. Clarke and D. A. Smith, Appl. Phys. Lett. **56**, 2396 (1990).
[20] M. Laguës, X. Hao and M. S. Dresselhaus, Phys. Rev. B **38**, 967 (1988).